



# Spatio-temporal variability of cloud cover types in West Africa with satellite-based and reanalysis data

Derrick Kwadwo Danso, Sandrine Anquetin, Arona Diedhiou, Christophe Lavaysse, Arsène Koba, N'Datchoh Evelyne Touré

## ► To cite this version:

Derrick Kwadwo Danso, Sandrine Anquetin, Arona Diedhiou, Christophe Lavaysse, Arsène Koba, et al.. Spatio-temporal variability of cloud cover types in West Africa with satellite-based and reanalysis data. Quarterly Journal of the Royal Meteorological Society, 2019, 145, pp.3715-3731. 10.1002/qj.3651 . hal-02327324

**HAL Id: hal-02327324**

**<https://hal.science/hal-02327324>**

Submitted on 30 Jun 2023

**HAL** is a multi-disciplinary open access archive for the deposit and dissemination of scientific research documents, whether they are published or not. The documents may come from teaching and research institutions in France or abroad, or from public or private research centers.



L'archive ouverte pluridisciplinaire **HAL**, est destinée au dépôt et à la diffusion de documents scientifiques de niveau recherche, publiés ou non, émanant des établissements d'enseignement et de recherche français ou étrangers, des laboratoires publics ou privés.



Distributed under a Creative Commons Attribution 4.0 International License

## RESEARCH ARTICLE

# Spatio-temporal variability of cloud cover types in West Africa with satellite-based and reanalysis data

Derrick Kwadwo Danso<sup>1,2</sup>  | Sandrine Anquetin<sup>1</sup> | Arona Diedhiou<sup>1,2</sup>  | Christophe Lavaysse<sup>1</sup> | Arsène Koba<sup>2</sup> | N'Datchoh Evelyne Touré<sup>2</sup>

<sup>1</sup>Université Grenoble Alpes, IRD, CNRS, Grenoble-INP, IGE, Grenoble, France

<sup>2</sup>Laboratoire de Physique de l'Atmosphère et de Mécaniques des Fluides (LAPAMF), Université Félix Houphouët, Abidjan, Côte d'Ivoire

## Correspondence

Derrick Kwadwo Danso, Université Grenoble Alpes, Institut des géosciences de l'environnement (IGE), CS 40700, 38058 Grenoble Cedex 9, France.  
Email: derrick.danso@univ-grenoble-alpes.fr

## Funding information

Institut de Recherche pour le Développement

## Abstract

This study aims to understand and document the occurrence and variability of cloud cover types in West Africa (WA). Investigations are carried out with a 10-year hourly record of two cloud data products: CERES passive satellite observations and ERA5 reanalysis. The seasonal evolutions of high (HCC), middle (MCC), low (LCC) and total (TCC) cloud cover are examined. Both products agree on the seasonal and spatial occurrence of cloud cover, although CERES presents lower values of cloud fraction than ERA5 which is partly attributed to the inability of the satellite sensor to detect optically thin clouds in the atmosphere. Southern WA is found to be cloudier than other parts of the region in all seasons with mean TCC fractions of 70 and 80% for CERES and ERA5 respectively during the monsoon season. In all seasons, the presence of LCC over large areas of the Sahel/Sahara region is noted in the CERES product. This could be due to a possible misinterpretation of Saharan dust as low clouds which may have thus, caused it to overestimate the occurrences and fractions of LCC over this region. Northern WA is associated with higher frequencies of no cloud occurrence events, unlike the south where cloudless skies are rarely observed. Furthermore, in southern WA, overcast conditions of LCC are observed for a significant number of times (up to 20% of the time during the rainy season in CERES and 40% in ERA5). The climatology of cloud cover presented in this study could be useful for the planning of solar energy projects.

## KEYWORDS

CERES, cloud cover, ERA5, occurrence frequency, variability, West Africa

## 1 | INTRODUCTION

Clouds have an important influence on various aspects of the Earth's radiative balance. Their presence modulates the incoming solar and outgoing long-wave radiation, surface temperature, and the Earth's atmospheric general circulation.

Cloud–radiation interaction is also responsible for a large degree of uncertainty in global climate models (GCMs) (Soden and Held, 2005; Dolinar *et al.*, 2014). A long-term observation of clouds is, therefore, necessary to understand the influence of clouds on the climate system. However, in West Africa (WA) a long-term observation of clouds is

This is an open access article under the terms of the Creative Commons Attribution License, which permits use, distribution and reproduction in any medium, provided the original work is properly cited.

© 2019 The Authors. *Quarterly Journal of the Royal Meteorological Society* published by John Wiley & Sons Ltd on behalf of the Royal Meteorological Society.

lacking, making it difficult to study the influence of clouds for many applications such as the ability to predict incoming surface solar radiation.

Cloud cover and its temporal evolution predominantly drive the variability of atmospheric reflectivity that determines the amount of solar radiation reaching the Earth's surface. Indeed, in a study by Supit and van Kappel (1998), information on cloudiness was used to estimate surface solar radiation at locations where there were no radiation measurements. Clouds when present, reflect, scatter and transmit parts of incoming solar radiation. Kasten and Czeplak (1980) found that the extent of reflection, scattering or transmission by clouds depends on the type of cloud and its characteristics. Knowledge of the types and variability of clouds is thus very crucial to understand their effects on the different components of the Earth's radiative budget.

In general, the WA region has a complex cloud cover system which ranges from low layered clouds associated with moisture flux coming from the Gulf of Guinea (van der Linden *et al.*, 2015), to deep mesoscale convective systems advected from east to west (Schumacher and Houze, 2006; Fink *et al.*, 2010) and local convection associated with the state of the continental surface (Sylla *et al.*, 2011). The interannual variability of these clouds has been found to be relatively small (Bouniol *et al.*, 2012) but some systems are known to be associated with intraseasonal variation due to the intermittency of the African Easterly Wave (Söhne *et al.*, 2008) or the variability of the Saharan Heat-low (Lavaysse *et al.*, 2010). In the rainy season (JJAS), cloud systems' occurrence in the region is greatly influenced by the West African Monsoon (WAM) (Klein *et al.*, 2015) with the more frequent occurrence and patchier structures in the afternoon (Söhne *et al.*, 2008). In the southern part of WA, there is a frequent occurrence of an extended cover of shallow low-level, non-precipitating stratiform clouds which often persist into the day, considerably reducing incoming surface solar radiation (Knippertz *et al.*, 2011).

Part of these different cloud systems mainly drive the variability of atmospheric reflectivity but remains poorly studied due to lack of a long-term consistent database of cloud cover observations. In addition, large differences exist between the different satellite, reanalysis and model datasets that are used in place of ground observations to study clouds in the region (Hill *et al.*, 2016). The contribution of cloud cover to the radiation budget is thus not very well understood in several parts of the region. A few regional field campaigns such as the African Monsoon Multidisciplinary Analysis (AMMA: Redelsperger *et al.*, 2006) and Dynamics-Aerosol-Chemistry-Cloud Interactions in West Africa (DACCWA: Knippertz *et al.*, 2015) have provided invaluable information on clouds in some parts of the region. Otherwise, ground-based observations of clouds are only available at the Atmospheric Radiation Measurement

(ARM) Mobile Facility (AMF) site in Niamey, Niger (Miller and Slingo, 2007). Most studies dealing with the influence of clouds on solar radiation in WA have therefore been limited to Niamey, in the Sahel region (e.g. Bouniol *et al.*, 2012; Bourgeois *et al.*, 2018).

Bouniol *et al.* (2012) identified four cloud classes in the Niamey region: low-level clouds (bases below 3 km), mid-level clouds (bases between 3 and 7 km), cirrus clouds (bases above 8 km) and deep convective systems. Mid-level clouds and anvil clouds (which are associated with deep convective systems) were found to have the largest impact on incoming solar radiation with radiative effects up to 150 and 300 W/m<sup>2</sup> respectively varying across months, whereas cirrus clouds were found to have a minimal impact on solar radiation, reducing surface radiation up to about 50 W/m<sup>2</sup>. Bourgeois *et al.* (2018), in a different study on the Niamey region, found that the cloud short-wave radiation effect ranges between −220 and −20 W/m<sup>2</sup> depending on the month and cloud properties. In some parts of southern WA, satellite observations have been used to show a large amount of incoming solar radiation is reflected back to space due to the presence of different cloud types (Hill *et al.*, 2018).

The space–time variability of most of these cloud types and convection are not well understood and documented in several areas of the WA region, thus leaving many open key questions when dealing with the variability of atmospheric reflectivity due to cloud cover. Within this context, the present study aims to understand and document the climatology of cloud cover in the WA region. While previous studies such as Hill *et al.* (2016; 2018) focus on cloud cover evolution in only southern WA, we first present a regional overview of cloud cover variability over the whole of WA in general and then focus on the variability of these clouds in different climatic zones over the region. We intend to provide different scales of variability for different cloud cover type occurrences in the region which could be important for understanding different components of the Earth's radiation budget such as the amount of incoming surface solar radiation.

The article is organised as follows: section 2 provides a description of the datasets and methodology. Section 3 presents and discusses the results of cloud cover variability in the region while the occurrence frequencies of clouds are presented and discussed in section 4. Conclusions are drawn in section 5.

## 2 | DATASETS AND METHODS

In this study, the time and space scales of variability of the cloud cover in WA are investigated from the perspective of evaluation of the solar energy resource. The present study, however, does not provide an evaluation of available solar energy resources. The cloud cover information comes from both European Centre for Medium-range Weather Forecasts

**TABLE 1** Summary of the different cloud cover variables of ERA5 and CERES data products used in this study

Variable name	Product variable definitions (by pressure levels)		Spatial resolution	
	CERES	ERA5	CERES	ERA5
Low-level cloud cover (LCC)	Surface to 700 hPa	Surface to 800 hPa	1° × 1°	Extracted at 1° × 1° (native horizontal resolution ~0.3°)
Mid-level cloud cover (MCC)	Lower mid-level clouds (700 hPa to 500 hPa)	800 hPa to 450 hPa		
	Higher mid-level clouds (500 hPa to 300 hPa)			
High-level cloud cover (HCC)	300 hPa to 50 hPa	450 hPa to TOA		
Total cloud cover (TCC)	Integration of all clouds from 50 hPa to surface	Integration of all clouds from TOA to surface		

The definitions of cloud cover type are based on the pressure levels. TOA refers to “top of the atmosphere”.

(ECMWF) reanalysis ERA5 (Copernicus Climate Change Service, 2017) and passive remotely sensed observations of the Clouds and the Earth's Radiant Energy System (CERES: Wielicki *et al.*, 1996), both at an hourly time-scale for a period of 10 years from 2006 to 2015. The analysis in this study allows the comparison and thus the identification of differences between the two cloud cover data products, both of which have not yet been used to study cloud systems in the WA region. As detailed in appendix S1, the two datasets were first evaluated against synoptic *in situ* observations of the Integrated Surface Database (ISD: Lott *et al.*, 2001) provided by the National Climatic Data Centre (NCDC). The evaluations revealed that differences in the magnitude of occurrence of sky cover classes between the synoptic *in situ* observations and ERA5 and CERES are not so large (Figure S1 in appendix S1).

## 2.1 | Datasets

### 2.1.1 | Reanalysis data

Hourly cloud cover fraction data from ERA5 were extracted on a regular 1° × 1° grid over WA. ECMWF's Integrated Forecasting System (IFS) implements the Tiedtke cloud scheme (Tiedtke, 1993) to forecast a three-dimensional (3D) cloud fraction, cloud liquid water and cloud ice water for each grid box. These cloud variables are produced in CY41R2 of the ECMWF's IFS and documented in Part IV of the IFS Documentation (available at <https://www.ecmwf.int/en/elibrary/16648-part-iv-physical-processes>).

ERA5 provides a 3D distribution of cloud cover parameters including cloud fraction, specific cloud liquid and ice water, prognostically computed at model levels as well as diagnostic cloud cover fractions on 2D single atmospheric layers (namely low-level, mid-level, high-level and total atmospheric column). The 2D cloud fraction variables include the total cloud cover fraction (TCC) which integrates

all clouds from the surface level to the top of the atmosphere with overlap assumptions (Jakob and Klein, 2000; Barker, 2008). Additionally, low-level (LCC), mid-level (MCC) and high-level (HCC) cloud cover fractions are respectively defined as the integration of all clouds from the surface to 800 hPa, 800 to 450 hPa and from 450 hPa to the top of the atmosphere (TOA) (Forbes, 2017). In this study, the 2D single-layer diagnostic cloud fractions are used for different analyses. Detailed documentation of the ERA5 data is provided at <https://confluence.ecmwf.int/display/CKB/ERA5+data+documentation>. Table 1 provides a summary of the cloud variables used.

### 2.1.2 | Satellite observations

Passive satellite sensor observations of cloud cover are extracted over WA from the hourly CERES SYN1deg Ed4A (Minnis *et al.*, 2016) product (hereinafter CERES). A combination of cloud properties measured by the MODerate-resolution Imaging Spectroradiometer (MODIS) sensor on board the Terra and Aqua platforms and geostationary satellite (GEO) images (Minnis *et al.*, 2011) are used to derive the CERES product. This product is intended for applications that require high temporally resolved (up to 1 h) information on cloud cover and for regional diurnal process studies (Atmospheric Science Data Centre – ASDC, 2017).

The MODIS and GEO cloud information which is contained in the CERES product is spatially and instantaneously averaged into 1° × 1° gridded regions at one-hourly intervals. Cloud cover information retrieved during the MODIS observation periods may be different from the surrounding GEO cloud cover information due to their retrieval differences.

The instantaneous gridded cloud cover fractions from the product are stratified by four pressure layers indicating



the pressure at the cloud top height and thus leading to four cloud cover types; surface–700 hPa (low-level clouds), 700–500 hPa (lower mid-level clouds), 500–300 hPa (higher mid-level clouds), and 300–50 hPa (high-level clouds). We use these cloud cover variables in addition to the total cloud layer which is simply the four-layer sum for a specific spatial and temporal resolution (Table 1).

The CERES sensors, like all passive sensors, have difficulty in identifying multiple cloud layers and are usually unable to detect low clouds that occur below a higher cloud. Active sensors are less prone to these issues and may provide a solution. However, most of the presently available actively sensed cloud products such as the very useful Cloud-Sat and Cloud–Aerosol Lidar and Infrared Pathfinder Satellite Observations mission (CALIPSO: Stephens *et al.*, 2018) do not provide a continuous high temporal resolution at a given location and may introduce some uncertainties when used for applications that require continuous high-resolution data. The CERES product used in this study removes this issue by providing instantaneous hourly information on clouds for more than a decade. Comprehensive information on the CERES product, including cloud retrieval algorithm, inputs and potential issues, has been already documented in ASDC (2017).

## 2.2 | Methods

The datasets used in the study have the same temporal resolution. However, the native horizontal resolution of ERA5 is approximately  $0.3^\circ$  but has been extracted directly at a  $1^\circ$  resolution, equal to the resolution of CERES. CERES provides two mid-level cloud layers (higher mid-level and lower mid-level) whereas ERA5 provides just one. In order to compare them, a representative single mid-level layer is computed by summing the two mid-level layers of CERES. It must be noted that definitions of the different cloud cover layers provided by the two products are slightly different (Table 1).

In this study, we look at both seasonal and diurnal climatologies of the three cloud types. At the synoptic scale (the whole WA region), the mean cloud cover fraction is determined for each northern hemispheric season (i.e. winter: DJF, spring: MAM, summer: JJA, and autumn: SON) by computing the mean of the instantaneous hourly cloud cover fraction values. In addition, the seasonal mean diurnal variability of each cloud cover type is determined for five equal-sized bounded windows across the region as shown in Figure 1 and detailed in Table 2. The windows in Niger, Burkina Faso, and Senegal are located in the Sahelian climate region (Gbobaniyi *et al.*, 2014) of WA. The other two windows are located in Benin and Côte d'Ivoire in the Sudanian and Guinean regions (Klein *et al.*, 2015) of WA respectively. Both the Senegal and Côte d'Ivoire windows share proximity

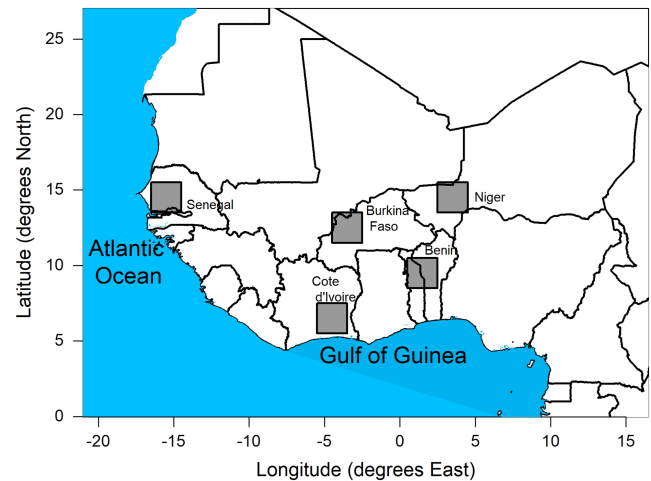


**FIGURE 1** Map of WA showing the five  $2^\circ \times 2^\circ$  bounded windows (grid boxes) selected for studying cloud variability at smaller space scale. The name assigned to each window is based on the country within which it lies. Niger, Burkina Faso and Senegal windows are located in the Sahelian climate region while Benin and Côte d'Ivoire are located in the Sudanian and Guinean climate regions respectively

to the ocean (Atlantic Ocean to the west for Senegal and the Gulf of Guinea to the south for Côte d'Ivoire). Their proximity to the ocean diversifies cloud formation processes such as the contribution of sea–land breeze circulation to cloudiness (Parker and Diop-Kane, 2017), absent in the other Sahelian region where cloud systems primarily arise from Mesoscale Convective Systems (MCS) (Vizy and Cook, 2018) advected from east to west. North of latitude  $15.5^\circ\text{N}$ , the mean cloud coverage is very low (Hill *et al.*, 2016), thus no window has been chosen in this part of WA.

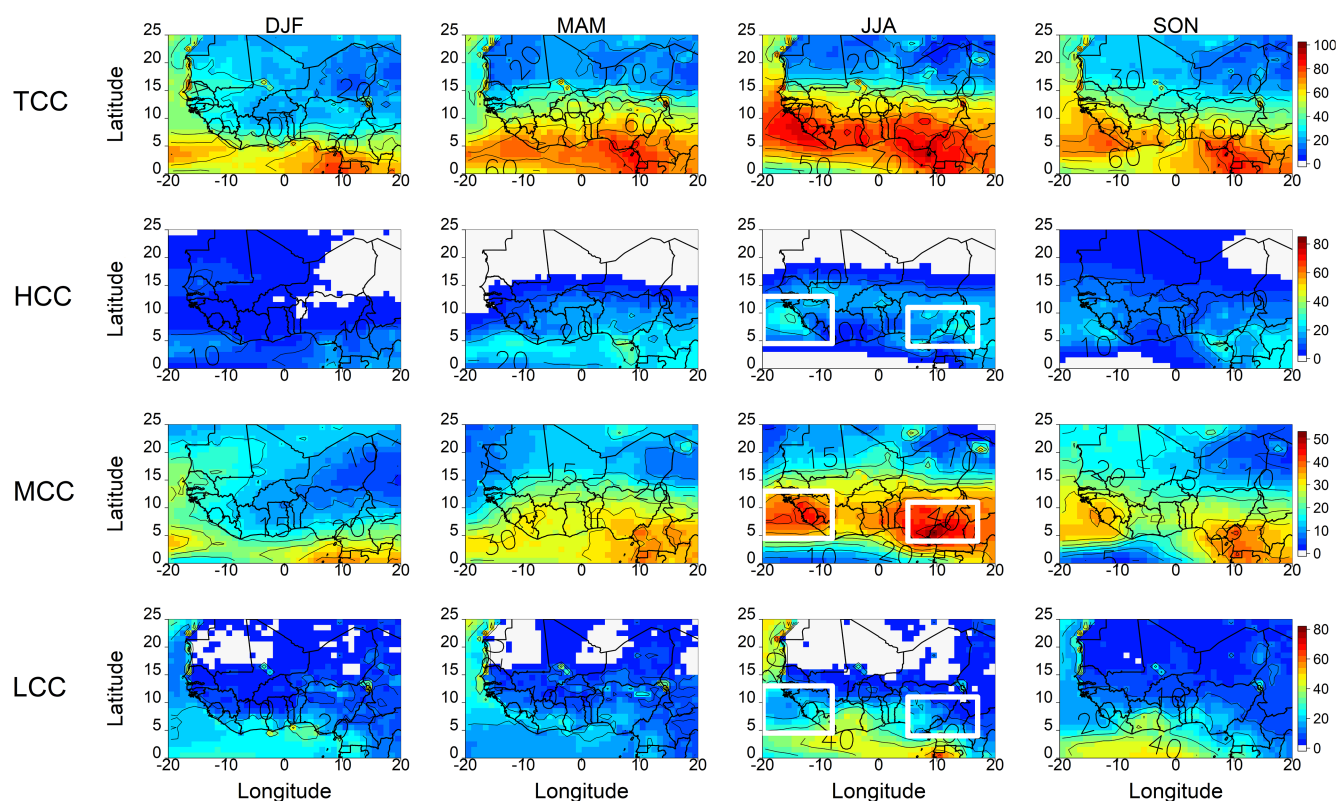
Due to the dependence of surface solar radiation on clouds, the occurrence frequency (Cai *et al.*, 2017) of cloud cover could be very useful to characterise, for example, fluctuations in incoming solar radiation received on solar panels in a given area. For the three cloud types being considered in the study, we computed (and compared) the occurrence frequency retrieved from the two datasets for only daytime hours (i.e. 0600 to 1700 UTC). Thus, the occurrence frequency is defined as the percentage of occurrences out of the total number of data records (i.e. 43,824 daytime hours for 10 years of records).

## 3 | CLOUD COVER VARIABILITY IN WA

In this section, we present a comparison of regional-scale, average daytime seasonal evolutions of cloud cover (i.e. total cloud cover and the three cloud types) determined from the satellite-derived CERES product and ERA5 reanalysis. We also present a comparison of the average diurnal evolutions of the cloud cover types for the two data products in some selected windows.

**TABLE 2** Geographical coordinates of the five equal-sized windows selected for analysing cloud cover occurrences and variability across WA

Window name	Longitude bounds (°E)	Latitude bounds (°N)	Climate zone
Côte d'Ivoire	−5.5° to −3.5°	5.5° to 7.5°	Guinean
Benin (and part of Togo)	0.5° to 2.5°	8.5° to 10.5°	Sudanian
Burkina Faso	−4.5° to −2.5°	11.5° to 13.5°	Sahelian
Niger	2.5° to 4.5°	13.5° to 15.5°	Sahelian
Senegal	−16.5° to −14.5°	13.5° to 15.5°	Sahelian

**FIGURE 2** Seasonal average evolutions of TCC, HCC, MCC and LCC in percentage of coverage over WA of CERES satellite-based cloud products. The contours on the figure show the average fractional coverage of each cloud category. The average values of cloud fractions shown here are computed from the hourly daytime (0600 UTC to 1700 UTC) values for a 10-year period (2006–2015). The white rectangles in JJA for HCC, MCC and LCC show areas where high HCC and MCC obscure the satellite sensor from detecting lower-lying clouds

### 3.1 | Seasonal evolution of cloud cover

Figures 2 and 3 show the seasonal distributions of TCC, HCC, MCC and LCC for CERES and ERA5 respectively. The evolution of TCC correlates well in the two products. In both products, higher coverage of clouds (greater than 40%) is found over the oceanic and coastal regions of WA during DJF season while the inner land areas have lower fractions of cloud coverage. ERA5, however, shows relatively higher coverage of clouds extending from the northwestern coast to some parts of the inner regions of Senegal, Mauritania and Mali. From the southern coast, TCC increases and extends into the inner regions beginning from MAM. Maximum coverage occurs during JJA after which there is a decrease in cloud coverage

in SON during which there is a shift of higher fractional coverage from the northern to the southern part of the region. Generally, the mean values of cloud coverage in ERA5 are slightly higher than in CERES.

The spatial and temporal occurrence of HCC and MCC are similar over the region in both products with both cloud types ubiquitous over the majority of the region throughout the year, while coverage strengthens during the monsoon season. However, the mean values of MCC are generally higher in CERES than in ERA5. Nevertheless, the mean values of HCC in CERES are much lower than the mean values in ERA5. This is perhaps explained by the difficulty of detecting optically thin cirrus clouds by MODIS as revealed by previous studies (e.g. Lee *et al.*, 2009; Sun *et al.*, 2011; Hill *et al.*, 2016), leading to

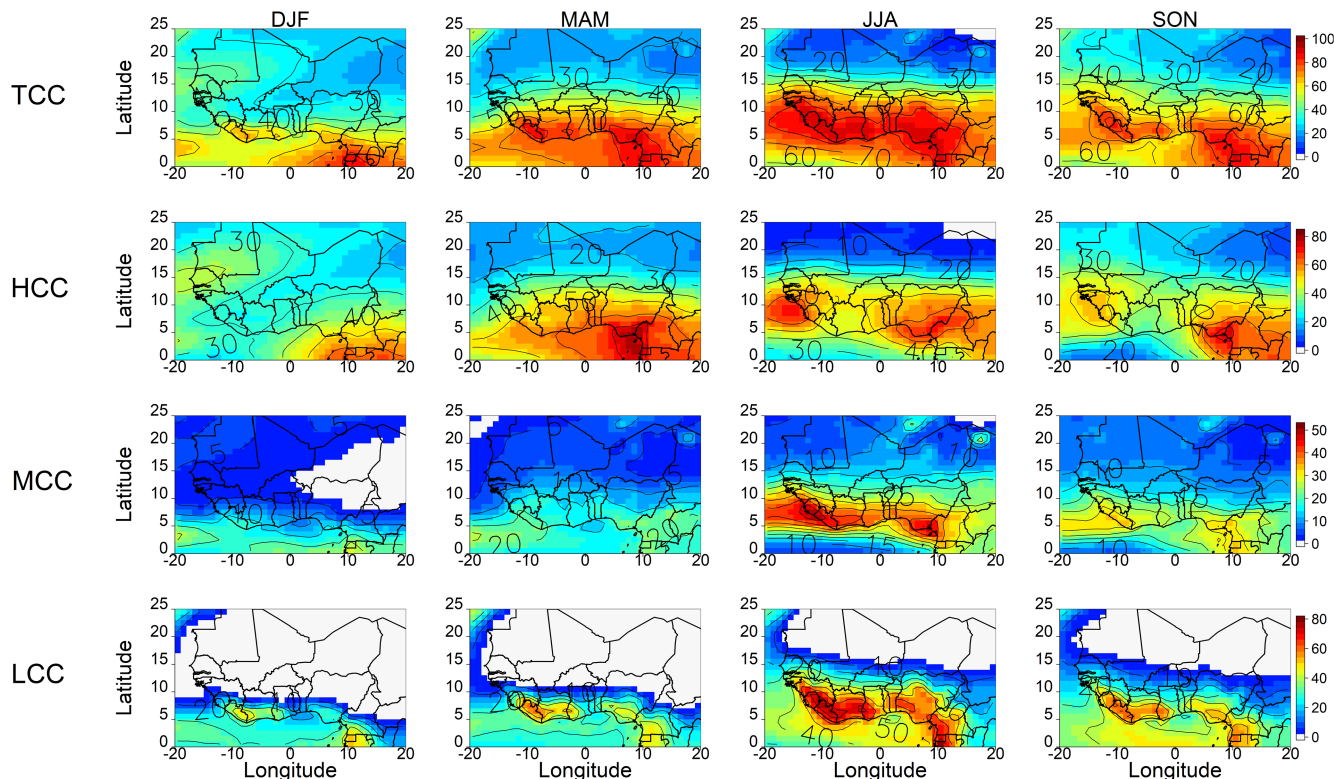


**FIGURE 3** Seasonal average evolutions of TCC, HCC, MCC and LCC in percentage of coverage over WA of ERA5 cloud products. The contours on the figure show the average fractional coverage of each cloud category. The average values of cloud fractions shown here are computed from the hourly daytime (0600 UTC to 1700 UTC) values for a 10-year period (2006–2015)

the lower mean fractions of HCC. The slightly lower values of TCC shown by CERES than ERA5 could be attributed to this same reason but needs to be investigated further. In addition, water vapour channels on Terra-MODIS experienced some degradation around 2008, thus affecting cloud retrievals (ASDC, 2017).

LCC coverage is also characterised by high seasonal variability, generally present in higher fractions only around the coastal regions during the dry season (DJF), after which the density of coverage extends northwards reaching a maximum during the monsoon season (JJA). In both products, there is a clear monsoon maximum of LCC coverage around the coastal regions of Côte d'Ivoire, Ghana and parts of Nigeria in agreement with van der Linden *et al.* (2015). The signal is, however, relatively stronger in ERA5 than in CERES. Passive satellite sensors are not able to detect low clouds when there are overlying clouds at higher altitudes (Karlsson and Johansson, 2013); this may explain the relatively low values of LCC fraction over the coastal areas (even during the monsoon season) for the CERES product. For instance, the highlighted areas in Figure 2 (white rectangles in JJA for HCC, MCC and LCC) show regions with high mean HCC and MCC. In the same regions for LCC, mean cloud fractions are relatively lower than in the surrounding areas.

During DJF and MAM, CERES does not show a well-marked spatial variability of LCC between the Guinean

(south) and Sahel/Sahara (north) regions. Surprisingly, CERES shows LCC over the Sahel/Sahara areas (up to about 20%) during the entire year, considering that low clouds (example shallow convective systems) rarely occur over these areas except in the core of the monsoon season (Bouniol *et al.*, 2012). A spatial gradient of low-level convection between the Sahelian and Guinean regions is thus expected due to the proximity of the latter to the ocean, leading to an influx of moisture from oceanic breezes and thus enhancing convection over these regions. This is however not the case in the CERES LCC seasonal evolutions (especially in DJF, MAM and SON). Considering that previous versions of CERES had struggled to discriminate between clouds and dust (ASDC, 2017; Loeb *et al.*, 2018), we suspect that dust particles over the Sahara could have been misinterpreted as LCC by the MODIS sensor, and CERES may have overestimated the presence of LCC over this region. Indeed, the local maxima of LCC found between Niger and Chad during DJF and SON seem to be an extension of the Bodélé depression (Middleton and Goudie, 2001; Koren *et al.*, 2006), an important dust source in the Sahara Desert. Other LCC local maxima can be seen during the year in other parts of the Saharan region, seeming to follow some dust sources in the region (Crouvi *et al.*, 2012; Knippertz and Todd, 2012).

While the spatial and temporal gradient of LCC is weaker in CERES, ERA5 shows stronger seasonal evolution and



clearer spatial gradients of LCC between the southern and northern parts of WA. The seasonal evolution of LCC could be linked to the seasonal displacements of the intertropical convergence zone (ITCZ), as also discussed by Bouniol *et al.* (2012). LCC is only present along the Guinea coast during the Sahelian dry season, strengthening and extending northwards during the monsoon season. During the monsoon season, ERA5 shows no LCC occurrence in large parts of the Sahara Desert (north of latitude 18°N). This behaviour may be linked to the failure of reanalysis products to efficiently represent (in this case underestimate) the northward shift of the WA Monsoon (WAM) as indicated by both Hill *et al.* (2016) and Thorncroft *et al.* (2011). Moreover, an underestimation of potential evapotranspiration in ERA5 over deserts as mentioned in the product documentation means that the model could be too dry to generate LCC in some cases. Nevertheless, ERA5 seems to give a better representation of the seasonal and spatial evolutions of LCC in the region.

### 3.2 | Diurnal evolution of the cloud cover types

The mean seasonal diurnal cycles of HCC, MCC and LCC are presented in Figure 4 for Côte d'Ivoire (Figure 4a) and Niger (Figure 4b). The grid boxes in Senegal and Burkina Faso presents similar cycles as that of Niger while the cycle in the Benin grid box is similar to Côte d'Ivoire. The cycles for these three grid cells have thus, not been shown. The mean diurnal cycle (bold lines in Figure 4) is computed from hourly, day and night, data for the 10 years (2006–2015) and for both CERES and ERA5 datasets. The 10-year variability of the cloud fraction diurnal evolution within each season is characterised by the 10th and 90th inter-percentile ranges (shaded regions) in Figure 4.

Generally, the diurnal variations of cloud fraction present an important spread around the mean values whatever the season, the cloud types or the regions. In both regions (Figure 4a,b), high-level clouds (HCC) present the largest intraseasonal variability in its diurnal cycle when compared to the ones associated with low and mid-level clouds across all seasons and for both products. For HCC, ERA5 presents a much more uniform spread during the day while CERES has a much higher spread during the night hours than the daytime.

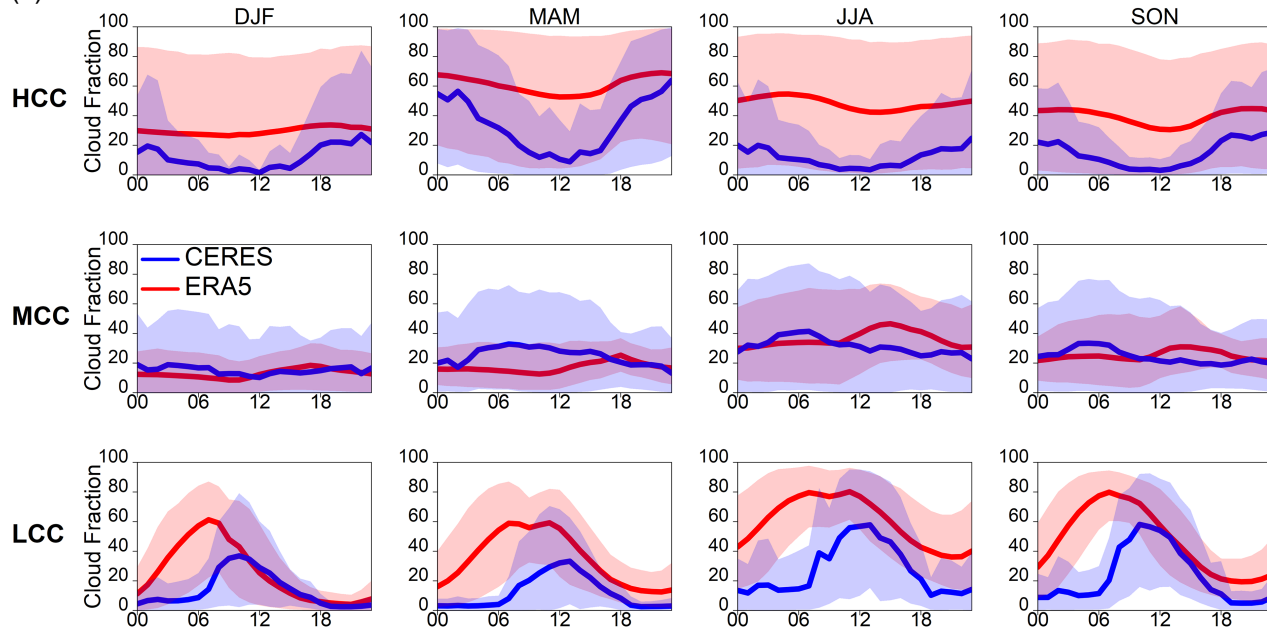
The HCC and MCC diurnal evolutions retrieved from the ERA5 dataset do not present any significantly marked diurnal cycle for average cloud fractions (thick solid lines) in both grid boxes. This absence of a well-marked diurnal cycle in ERA5 is unexpected considering the presence of distinctly marked diurnal cycles of HCC and MCC in previous studies (e.g. Hill *et al.*, 2016; Bourgeois *et al.*, 2018). CERES, however, shows some diurnal variation of HCC (but not for MCC) in both regions with higher cloud fractions in the night than during the day, more consistent with some previous studies in

the region (e.g. Bouniol *et al.*, 2012; Hill *et al.*, 2016). The diurnal cycle of HCC in CERES could be linked to the development of convection during the daytime (Stein *et al.*, 2011) and their consequent detrainment into anvil and cirrus clouds (Mace *et al.*, 2005; Sassen *et al.*, 2009) in the evening and night-time. This is however missed by ERA5 and is likely due to the convective parametrization (Bechtold *et al.*, 2013) used in the forecasts.

The LCC diurnal cycles present different patterns. In the Côte d'Ivoire box, LCC retrieved from both datasets have a very strong diurnal evolution for all seasons. ERA5 presents an early morning peak (around 0600 UTC) for fractional coverage while the CERES dataset provides an afternoon peak (around midday). Considering the closer proximity of the Côte d'Ivoire box to the ocean, the diurnal evolution of the ERA5 product seems to be consistent with the diurnal cycle of the tropical lower-level convection which generally reaches a maximum in the early morning in the oceanic and coastal areas (Yang and Slingo, 2001). The maximum fractions of HCC occur during the night-time (until the early morning) and obscure the CERES sensors from properly detecting low-lying clouds in range. This may explain the gap between the peaking periods of LCC in the two datasets. In addition, it appears night-time stratus decks in the region as revealed by van der Linden *et al.* (2015) are missed by the CERES product (very low or no LCC values at night in CERES relative to ERA5). This observation could also be attributed to the inability of CERES sensors to detect LCC at night when HCC is maximum and obscures the passive sensors. Additionally, lack of temperature contrast between warm surfaces and low clouds at night makes it difficult for passive sensors (CERES in this case) to detect LCC during the night (Knipertz *et al.*, 2011; van der Linden *et al.*, 2015; Andersen and Cermak, 2018).

For the Niger box, important differences exist between the two products. Firstly, CERES shows fractions of LCC in all seasons with no clearly marked diurnal cycle while ERA5 reveals the occurrence of LCC only during JJA, peaking around midday. The presence of LCC in all seasons for CERES can partly be linked to the presence of dust in the Sahel/Sahara areas which may be misinterpreted as clouds by the passive sensor as already discussed in section 3.1. The afternoon peak of LCC in ERA5 during the monsoon is consistent with the evolution of continental mesoscale convective systems (MCS) (Vizy and Cook, 2018). These MCSs, moving from east to west, are responsible for the majority of the clouds occurring in the Sahelian region during the monsoon season in WA. This also explains the difference in timing of the peak occurrence of LCC (for ERA5) in the two regions, i.e. 0600 UTC for Côte d'Ivoire, 1200 UTC for Niger. To a lesser extent, the differences in definitions of the cloud types for the two products could perhaps explain some of the differences between the two products.

## (a) Côte d'Ivoire



## (b) Niger

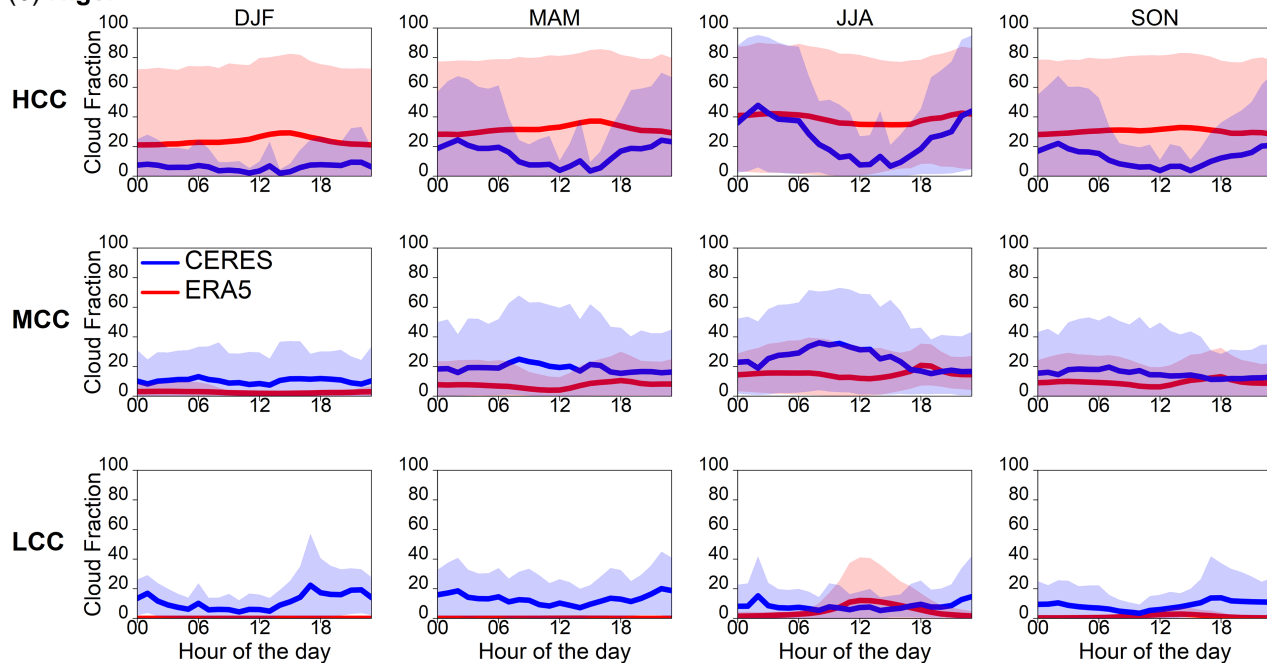


**FIGURE 4** Seasonal average diurnal evolution of cloud fraction (in percentage of coverage) of high (HCC), mid- (MCC) and low (LCC) level clouds provided by CERES satellite-based and ERA5 reanalysis for two among five selected boxes in (a) Côte d'Ivoire and (b) Niger. The shaded regions bounding the mean cloud fraction curves (solid lines) represent the 10th and 90th inter-percentile range in the diurnal evolution of cloud cover fractions

## 4 | CLOUD OCCURRENCE FREQUENCY IN WEST AFRICA

In this section, we present a 10-year climatology of cloud occurrence frequency under different perspectives. The cloud occurrence frequency is an important parameter to consider during the feasibility assessment for large-scale solar energy development. It could, for example, be used to characterise

the fluctuations of surface solar radiation received on solar panels due to cloud cover. Here we look at the occurrence frequencies of clouds in WA from a general perspective and then for each cloud type. The occurrence frequency is principally expressed as a percentage of events of specific interest ( $n$ ) relative to the total number of data observations ( $N$ ), where  $N$  is equal to 43,824 h, i.e. the total number of the defined day-time hours (between 0600 and 1700 UTC) from 2006 to 2015.



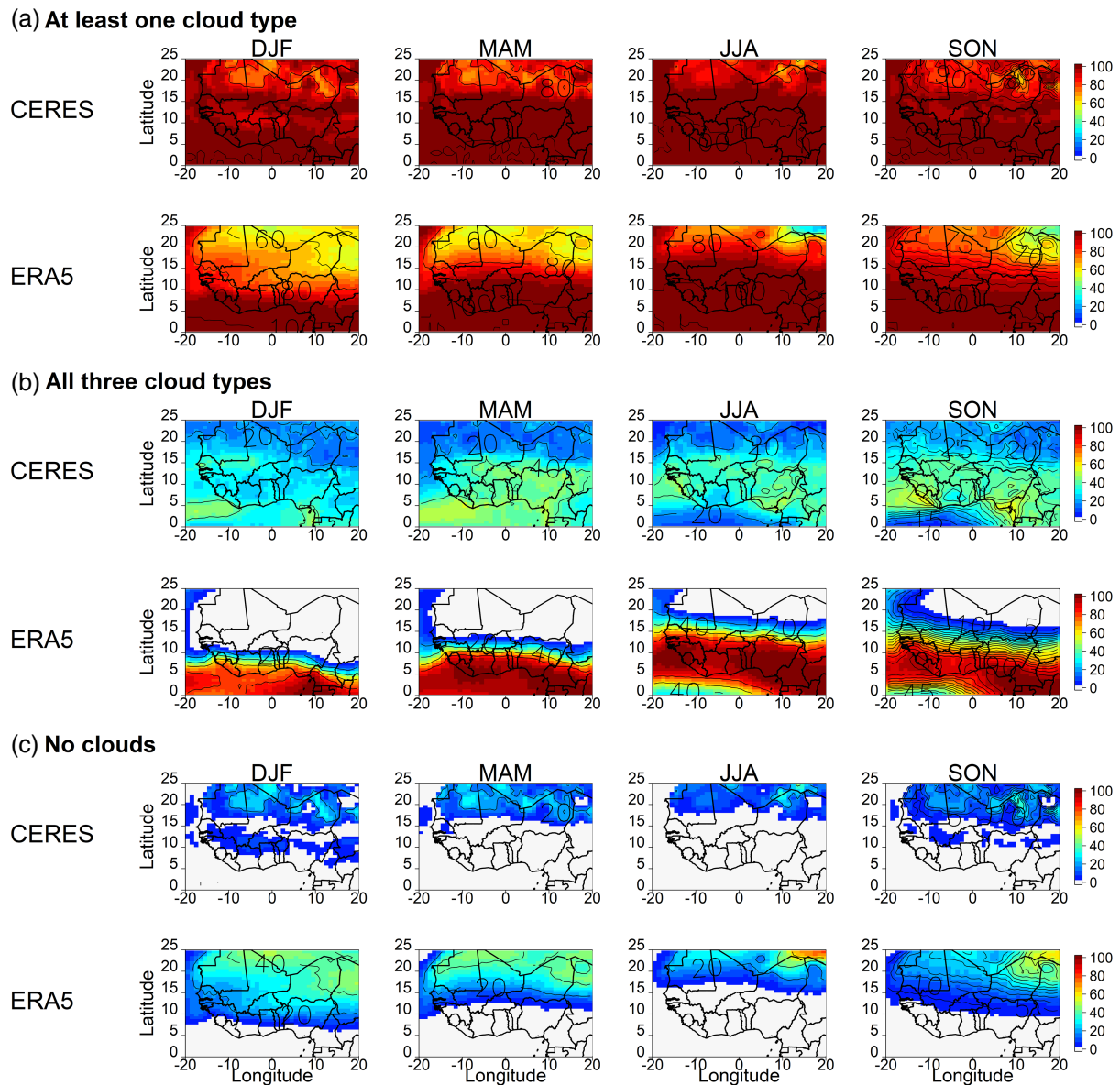


**FIGURE 5** CERES and ERA5 climatologies of occurrence frequency (representing the % of occurrence out of total observations in each season) for (a) at least one cloud type presence, (b) all three cloud types simultaneously and (c) no cloud presence, over WA

#### 4.1 | General occurrence frequency of clouds

Figure 5 shows the frequencies of at least one cloud type occurrence, the simultaneous occurrence of all three cloud types and no cloud occurrence in the whole WA region for each season. These occurrence frequencies have been computed for both cloud products without taking into account the magnitude of cloud fraction.

The frequency of having at least one cloud type occurring (Figure 5a) generally decreases from south to north in both products and for all seasons. Additionally, JJA has a higher frequency of at least one cloud type occurrence in a lot of areas in the region relative to other seasons. In JJA, both products reveal a 100% frequency of at least one cloud type occurrence (i.e. a cloud is always present)

in all areas south of latitude 15°N. Northwards of this latitude, frequencies are below 100% and decrease down to about 60% for ERA5 and 80% for CERES. In other seasons, the frequencies are rather lower in a lot of areas in the region. For example, during DJF in both products, only areas south of about 7°N (southern coastal region) experience 100% frequency for at least a cloud to be always present while all areas northwards of this latitude have lower frequencies (down to 80% for CERES and 60% for ERA5). The relatively higher values of CERES than ERA5 north of latitude 15°N in all seasons could be explained by dust being misinterpreted by the CERES sensor as already discussed in section 3.1. In the ERA5 product, there is a northward progression of the latitude, south of which all areas experience a 100% frequency of at least one cloud type occurrence

from DJF, peaking in JJA and shifting southwards again in SON. This seasonal evolution could be linked to the evolution of the WAM. Since the magnitude of cloud fraction is not taken into account, the computed frequencies encompass cloudiness of all ranges including very small cloud fractions which might not be easily visible to humans or certain instruments.

Figure 5b also shows the frequency of all three cloud types occurring at the same time over the region (regardless of the cloud fraction) for each season. Both products agree on the spatial distribution of frequency of the simultaneous occurrence of all three cloud types but there are pronounced differences in terms of the magnitude of the frequencies. While there is a distinct northward progression of the frequency maxima from DJF to JJA and a slight southward shift in SON in the ERA5 product, the CERES product does not reveal a well-marked seasonal evolution of these frequency maxima shifts. Moreover, in all seasons, CERES shows that all three cloud types occur at the same time between 20 and 30% of the time in the Sahel/Sahara areas and up to about 50% of the time in southern WA (south of 10°N). ERA5, however, reveals a 0% occurrence frequency in areas north of 10°N in DJF and north of 15°N in MAM (all areas below these latitudes have frequencies ranging from 10 to 90%). In JJA and SON, only the northern parts of Mauritania, Niger and Mali have a 0% frequency of all three clouds occurring at the same time.

Figure 5c presents the frequency of no cloud occurrence in the WA region. While only a few coastal areas in southern WA have 0% frequency of no cloud occurrence in DJF for both products, a large portion of WA (all areas south of latitude 15°N) in JJA has a 0% no clouds occurrence frequency. This is due to the influx of moisture from the Gulf of Guinea during the active monsoon season, enhancing cloud formation over those areas. CERES shows relative lower frequencies of no cloud occurrence in northern WA across all seasons than ERA5. This could be attributed to dust particles that are misinterpreted as low clouds by the sensor even in the absence of real clouds and thereby reducing the frequency of events of no cloud occurrence.

The probability density plots of cloud fraction in Côte d'Ivoire (Figure 6a) reveals that the CERES product has a much higher number of events of zero fractions (no cloud cover) for all three cloud types than ERA5. This subsequently reduces significantly the number of possible events for simultaneous occurrence of all three cloud types, leading to a much lower frequency of all three cloud types occurring simultaneously near the Guinean coast by the CERES product. On the other hand, in the Sahel (Figure 6b, Niger box), ERA5 presents more zero cloud fraction events than CERES for MCC and LCC (extremely high for low clouds). This explains the slightly higher frequencies of simultaneous occurrence of all three clouds, north of the Sahelian region by the CERES product.

## 4.2 | Low-level cloud cover occurrence as a function of fractional coverage

LCC are known to have an important influence on the short-wave component of the radiation budget (Bouniol *et al.*, 2012; Pyrina *et al.*, 2013) depending on their thickness, fraction and water content (Liou, 2002). Thick low-level stratus and cumulus clouds block a large proportion of incoming solar radiation from reaching the Earth's surface. In this section, we present the frequency of low-level clouds occurrences in WA as a function of their fractional coverage. We classified LCC occurrence events into three classes depending on the cloud fraction (CF, %) value. The three-class definitions are: low coverage ( $0 < CF < 40$ ), moderate coverage ( $40 \leq CF < 80$ ) and high coverage/overcast ( $CF \geq 80$ ). Figure 7 presents the occurrence frequency for the three fractional coverage classifications of LCC (even when other cloud types are present) identified for all seasons in WA for the two products.

Over the entire region, the frequency of low coverage LCC is generally greater than moderate coverage LCC, which in turn is also greater than high coverage/overcast LCC. For low coverage of LCC (Figure 7a), CERES reveals a relatively less pronounced seasonal evolution of occurrence frequencies with values of at least 40% over the whole region. In all seasons, areas south of latitude 17°N have higher frequencies of low-coverage LCC than areas northwards of this latitude. ERA5, however, reveals a more pronounced seasonal evolution of low-coverage LCC with peak values progressing northwards from DJF to JJA (begins to shift southwards in SON). In DJF, almost the entire Sahel/Sahara regions have 0% frequency of low-coverage LCC (as well as moderate and high coverage LCC). But in JJA and SON, only parts of northern Mauritania, Mali and Niger experience 0% occurrence of LCC.

Both products also reveal a reduction of low-coverage LCC occurrence frequencies during JJA in southern WA (notably at areas closer to the coast). During the active monsoon season, the influx of moisture from the Atlantic Ocean enhances convection and thus LCC formation. The fractional coverage of LCC, therefore, increases, hence reducing the occurrence of low-coverage LCC during this period. This is however not the case when moderate and high/overcast coverage LCC are considered (see JJA for Figure 7b,c) as the enhancement of convection development increases the fractions of LCC in the lower altitudes.

Moderate coverage of LCC (Figure 7b) is mostly confined to the coastal southern WA up to about 10% in CERES and 20% in ERA5 during DJF and MAM. In JJA and SON, moderate coverage LCC occurrence increases at the coastal areas of southern WA (up to about 60% in ERA5 and up to about 40% in CERES) and progresses to just south of the Sahelian region (south of latitude 15°N in ERA5 but also some other

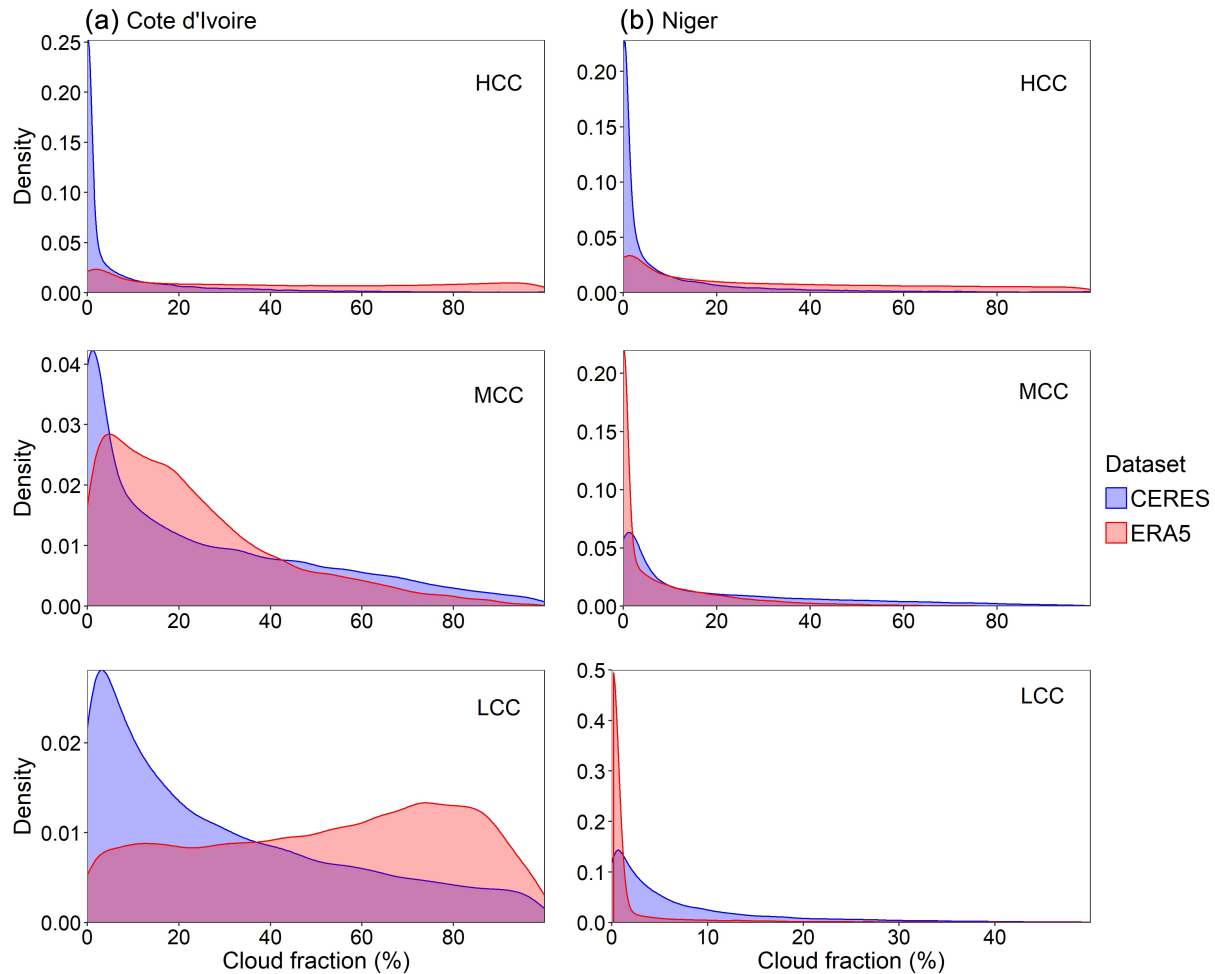


**FIGURE 6** Probability density distributions of high-level (HCC), mid-level (MCC) and low-level (LCC) cloud fractions retrieved from the CERES and ERA5 datasets and for (a) the Côte d'Ivoire box and (b) the Nigerien box. This distribution is only generated from daytime hours between 0600 UTC and 1700 UTC

areas in the Sahara region in CERES). In the same way, it is more common to observe high fractional coverage or an over-cast condition (Figure 7c) of low-level clouds near the coastal regions of southern WA rather than in northern WA where such occurrences are very rare or non-existent in JJA and SON. In addition, the ERA5 product shows slightly higher frequencies than the CERES product over the coastal areas of southern WA when moderate and high coverage LCC are considered.

### 4.3 | Solitary occurrence of cloud types

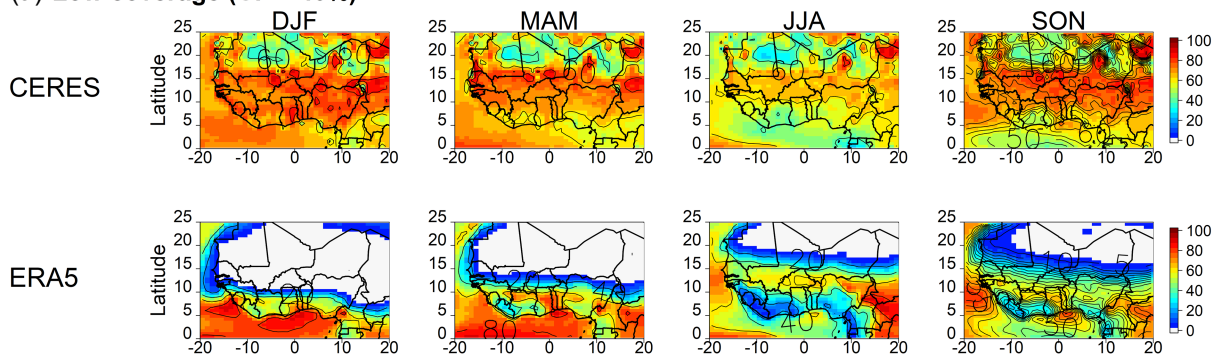
To determine the radiative effect of a particular cloud type (not done in the present work), it is necessary to consider only events of lone occurrence of that cloud type, i.e. without the presence of other cloud types. For the two data products, we therefore computed the occurrence frequency of each cloud type when no other cloud types were present in all seasons. In these computations, we did not take into account the cloud fraction. The results are illustrated in

Figure 8 and present important discrepancies between the two products especially for both LCC-only and HCC-only occurrences.

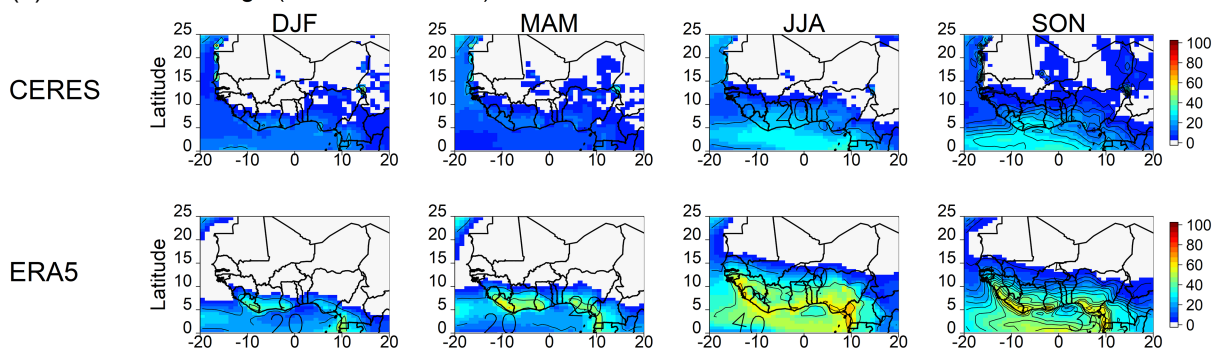
For LCC only (Figure 8a), CERES reveals occurrences with frequencies up to about 50% over the land areas of the region (except around some parts of southwestern Nigeria in JJA with 0%). ERA5, on the other hand, reveals that the occurrence of LCC only in the absence of other clouds is very rare over the land areas in WA except in some parts of southern WA closer to the coast in DJF. The higher values shown by CERES can be linked to the misrepresentation of dust as LCC as already discussed in section 3.1. Additionally, MODIS classifies very thin HCC over thicker LCC as low clouds (Hill *et al.*, 2016) due to its inability to detect the former and may have increased LCC-only frequency.

For the MCC-only occurrence (Figure 8b), the two products are in a relatively better agreement with just slight differences unlike for LCC only and HCC only. Both show a regional maximum occurrence in the northern part of WA (north of 15°N except in DJF in ERA5).

## (a) Low coverage (CF &lt; 40%)



## (b) Moderate coverage (40% ≤ CF &lt; 80%)



## (c) High coverage/ overcast (CF ≥ 80%)

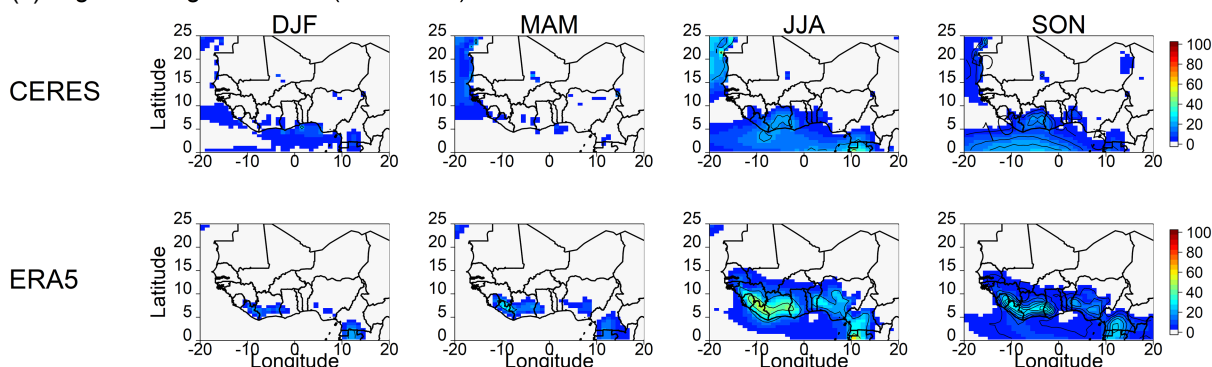


**FIGURE 7** CERES and ERA5 climatologies of occurrence frequency of low-level cloud occurrence (% of occurrence out of total time in each season) as a function of fractional coverage: (a) low coverage, fractions less than 40% (excluding 0%), (b) moderate coverage, fractions between 40 and 80%, and (c) high coverage or overcast, fractions higher than 80%

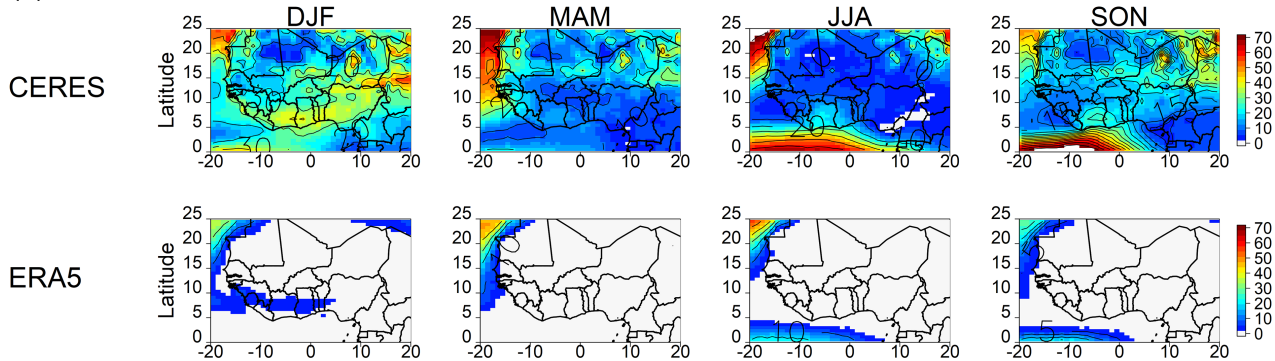
For HCC-only occurrence (Figure 8c), there are important differences between the two products. Generally, the CERES product has much lower frequencies than ERA5 and in addition, the number of areas with HCC-only occurrence increases from DJF to SON in CERES while it decreases from DJF to JJA, increasing again in SON. For example, in DJF CERES reveals a 0% frequency of HCC-only occurrence over almost the whole region while ERA5 shows frequencies up to about 60% (just a small area on the southern coast has 0% frequency). The 0% frequency shown over the entire WA by CERES could be partly due to the presence of LCC (dust misinterpreted as LCC) over the region but also the inability of the CERES sensor to detect very thin HCC in the atmosphere thereby missing many events of HCC-only occurrence.

In MAM, a similar occurrence is observed for both products but with reduced frequencies for ERA5 (with the area of 0% also shifting northwards) and also very low frequency values occurring at few areas over the Saharan region and Gulf of Guinea in the CERES product.

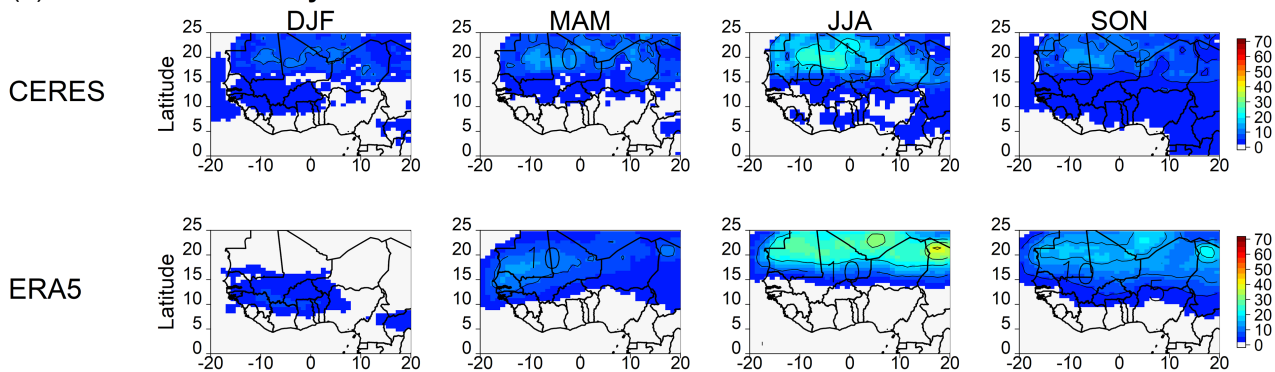
For ERA5 in JJA, all areas south of latitude 13°N have 0% frequency for HCC-only occurrence and all areas north of this latitude have relatively lower frequencies than in other seasons. This could be linked to the relationship between HCC formation and daytime convection. The vertical development of LCC and consequent detrainment at higher altitudes leads to the formation of HCC. The presence of HCC only is likely to be less considering that at the time of HCC formation, lots of LCC could still exist in the lower altitudes of the



## (a) Low-level clouds only



## (b) Mid-level clouds only



## (c) High-level clouds only

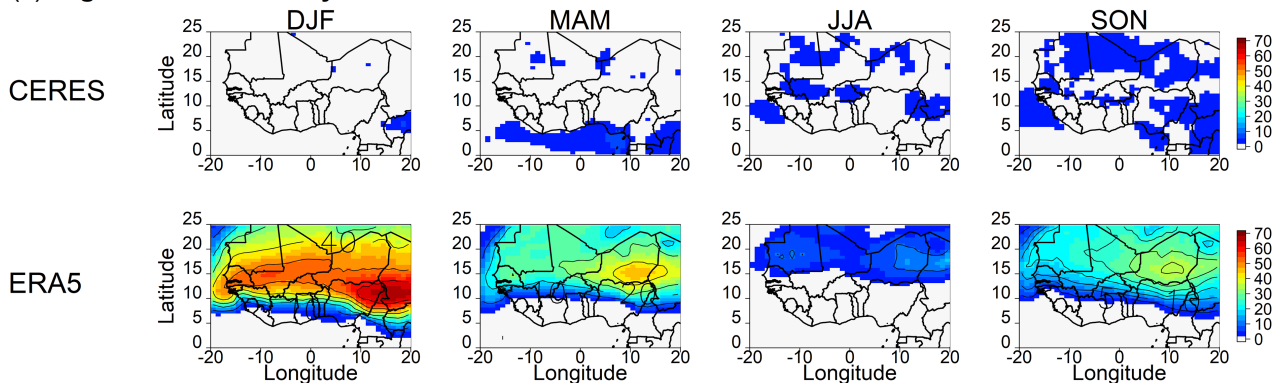


**FIGURE 8** CERES and ERA5 climatology frequencies of cloud occurrence (% of occurrence out of total time in each season), for each cloud type: (a) LCC, (b) MCC, (c) HCC, when the other clouds are not present

atmosphere (especially since we have considered only daytime hours for this computation). Low frequencies can be seen in a few places over the region in the CERES product.

The large discrepancies observed between the two products for LCC-only and HCC-only occurrences needs to be investigated further for better understanding. The interpretation of Figure 8, however, needs to be made with caution. For example, it might not be surprising that CERES has a higher occurrence frequency of LCC only since they can only be detected by the satellite instruments if there are no optically thick higher-level clouds. Additionally, the possible misinterpretation of dust as LCC could increase their occurrences.

## 5 | SUMMARY AND CONCLUSIONS

In this study, we examined the variabilities and the occurrences of cloud cover in WA, which could be essential for any feasibility study of solar energy potential in this data-scarce region. We developed and compared a 10-year climatology of different cloud types in WA from two cloud products: the satellite-derived CERES SYN1deg and ERA5. Four main outputs of the two products including TCC, HCC, MCC and LCC were used to document the regional-scale daytime seasonal evolutions and occurrence frequencies of cloud cover in WA. In addition, we presented the diurnal cycle of cloud cover fraction at grid-scale level for two selected equal-sized



bounded windows across the Sahelian and Guinean climate zones of the WA region.

To an extent, both products agree on the spatial distribution of cloud cover over the region but with some differences in the magnitude of the fractional coverage. As expected, the southern part of WA is much cloudier in all seasons and receives less incoming solar radiation than the other parts of the region. TCC in the region intensifies during the monsoon season (JJA) and is very intense in southern WA where mean cloud fractions are up to 70% for the CERES product and up to 80% for ERA5. In the Sahelian and northern parts of the region, TCC fractions are much lower (less than 50%) during the core of the monsoon. The CERES product reveals much lower magnitudes of cloud fraction than ERA5 for the three cloud types even though the spatial distributions seem to be fairly correlated. This behaviour is linked to the inability of the CERES sensors to detect optically thin HCC and MCC which occur in the region as well as the inability of passive sensors to detect low-lying clouds in multi-layered cloud cover events. In the ERA5 product, the seasonal evolution of LCC could be interpreted as being related to the seasonal movements of the ITCZ. This is, however, not readily noticeable in the CERES product, showing LCC over the entire region with a very little spatial gradient (except in JJA and SON). This behaviour is attributed to the difficulty of discriminating between dust and clouds by CERES, hence misinterpreting dust as LCC over the Sahelian and Saharan areas.

The seasonal evolutions of the diurnal cycle for cloud fraction of the three cloud types have been investigated for five selected boxes: Côte d'Ivoire, Benin, Burkina Faso, Niger and Senegal. For the sake of brevity, only the Ivorian and Nigerien (relating to Niger) contrasted regions are discussed in this article. In the Ivorian and Nigerien regions, no clear diurnal variation is detected in the HCC and MCC evolutions provided by the ERA5 datasets. CERES, however, has a relatively marked diurnal variation for HCC (but not for MCC) with lower (higher) fractional coverage during the day (night), more consistent with previous studies (e.g. Bouniol *et al.*, 2012; Hill *et al.*, 2016). LCC have a much significantly marked diurnal variation for both products in the Ivorian region. In the Nigerien area, CERES does not reveal any clear cycle while the ERA5 product presents a clear diurnal cycle mainly in the monsoon season. With the ERA5 dataset, the evolution of the LCC fractions presents a peak in the morning (around 0600 UTC) in the Ivorian region and around midday in the Nigerien area. This pattern is not replicated when the CERES dataset is used since we observe a shift to midday for the peak in Côte d'Ivoire and no clear cycle in Niger. The pattern of the diurnal variation provided by ERA5 is consistent with Weather Research and Forecasting (WRF) model simulations of Vizy and Cook (2018) and multi-satellite analysis of Yang and Slingo (2001) where an early morning peak for

tropical lower-level convection at coastal/oceanic areas and a midday to evening peak of Mesoscale Convective Systems are explicitly pointed out.

We also investigated the daytime occurrence frequency of clouds in the region based on several criteria for each season. Generally, the middle and northern parts of the region (north of latitude 10°N) are associated with high frequencies of no cloud occurrence events (frequencies for no cloud occurrence are much higher in ERA5 – up to about 50% than in CERES – up to about 20% of the time). South of a given latitude (e.g. 15°N for both products in JJA) there is at least one cloud type occurring at all times (we do not consider the magnitude of cloud fraction in this assessment). Additionally, all three cloud types can occur at the same time at a given location. The frequency of simultaneous occurrence of all three cloud types is much higher south of latitude 15°N but is considerably higher in ERA5 (up to 90% in some coastal areas) than in CERES (up to 40%) with reasons for such huge discrepancies already mentioned in the preceding paragraphs.

Considering the radiative effect of low clouds (i.e. thick stratocumulus and cumulus clouds) to incoming short-wave radiation and the dependence of the radiative effect on cloud cover extent, we expanded our investigations to occurrence frequency of LCC, taking the fractional coverage into account. The coastal areas of southern WA experience the highest occurrence frequencies of overcast conditions (coverage more than 80%) of LCC, i.e. up to 10% in CERES and 20% in ERA5. Along with the high frequencies of simultaneous occurrence of all three clouds, potential solar photovoltaic (PV) plants in this region are likely to produce a very low percentage of their nominal capacities for a significant number of times during the year (especially in the monsoon season due to the high reflectivity of the sky caused by clouds). Potential large-scale PV plants, therefore, require meticulous planning on plant sizing and/or distribution and number additional backup sources to cope with the potentially extreme fluctuations in power production.

The present study, therefore, provides comprehensive documentation of cloud occurrences and variability which could be extremely useful for planning large-scale solar energy projects in such a data-scarce region. Comparisons between the two datasets used have also been used to identify discrepancies, agreements and possible drawbacks in each product. Individually, each of the two products has its strengths and uncertainties and can be used to complement each other for planning purposes. For instance, the diurnal cycle of HCC appears to be represented well by CERES product while the seasonal and diurnal cycles of LCC seems to be captured well in ERA5. The two datasets also agree on the seasonal variability of TCC and at least the spatial distribution of some occurrence frequencies.

Nevertheless, the study reveals some important differences between the two datasets used, starting with the cloud

definition itself. The need for a high-quality and continuous database of cloud observations at high temporal resolution is thus imperative. Additionally, the study highlights the need to improve cloud retrieval algorithms in future CERES updates or planned satellite missions and to improve the microphysics schemes and parametrizations used in reanalysis products like ERA5. With a quality database of cloud observations in the region, this study lays out a blueprint for future assessment of solar energy development feasibility.

Future studies will be centred on identifying conditions for the occurrence of some cloud types (with datasets such as the state-of-the-art regional climate models for the region) and their associated short-wave radiative effect.

## ACKNOWLEDGEMENTS

We would like to deeply thank the two anonymous reviewers for their constructive comments and suggestions to strengthen this article. The research leading to this publication was made possible through support provided by the IRD-DPF (Institut de Recherche pour le Développement, France). The SYN1deg satellite-based cloud cover data were obtained from the Clouds and the Earth's Radiant System (CERES) webpage ([http://ceres.larc.nasa.gov/order\\_data.php](http://ceres.larc.nasa.gov/order_data.php)). ERA5 cloud cover data were obtained from European Centre for Medium-Range Weather Forecasts (ECMWF) webpage (<https://cds.climate.copernicus.eu/cdsapp#!/home>). We reserve special appreciation to Siélé Silué for his assistance on satellite data analysis during this study. We will also like to thank Adama Bamba and Kouakou Kouadio for their general comments on the study.

## ORCID

Derrick Kwadwo Danso  <https://orcid.org/0000-0001-7141-7530>

Arona Diedhiou  <https://orcid.org/0000-0003-3841-1027>

## REFERENCES

- Andersen, H. and Cermak, J. (2018) First fully diurnal fog and low cloud satellite detection reveals life cycle in the Namib. *Atmospheric Measurement Techniques*, 11, 5461–5470. <https://doi.org/10.5194/amt-11-5461-2018>.
- Atmospheric Science Data Center - ASDC. (2017) *CERES SYN1deg Ed4A Data Quality Summary*. Available at: <https://ceres.larc.nasa.gov/dqs.php#level3table> [Accessed 12th December 2018].
- Barker, H.W. (2008) Representing cloud overlap with an effective decorrelation length: an assessment using CloudSat and CALIPSO data. *Journal of Geophysical Research*, 113(24), 1–17. <https://doi.org/10.1029/2008JD010391>.
- Bechtold, P., Semane, N., Lopez, P., Chaboureaud, J.-P., Beljaars, A. and Bormann, N. (2013) Representing equilibrium and nonequilibrium convection in large-scale models. *Journal of the Atmospheric Sciences*, 71(2), 734–753. <https://doi.org/10.1175/jas-d-13-0163.1>.
- Bouniol, D., Couvreur, F., Kamsu-Tamo, P.H., Leplay, M., Guichard, F., Favot, F. and O'Connor, E.J. (2012) Diurnal and seasonal cycles of cloud occurrences, types, and radiative impact over West Africa. *Journal of Applied Meteorology and Climatology*, 51(3), 534–553. <https://doi.org/10.1175/JAMC-D-11-051.1>.
- Bourgeois, E., Bouniol, D., Couvreur, F., Guichard, F., Marsham, J.H., Garcia-Carreras, L., Birch, C.E. and Parker, D.J. (2018) Characteristics of mid-level clouds over West Africa. *Quarterly Journal of the Royal Meteorological Society*, 144(711), 426–442. <https://doi.org/10.1002/qj.3215>.
- Cai, H., Feng, X., Chen, Q., Sun, Y., Wu, Z. and Tie, X. (2017) Spatial and temporal features of the frequency of cloud occurrence over China based on CALIOP. *Advances in Meteorology*, 2017, 11. <https://doi.org/10.1155/2017/4548357>.
- Copernicus Climate Change Service (C3S). (2017). *ERA5: fifth generation of ECMWF atmospheric reanalysis of the global climate*. Copernicus Climate Change Service Climate Data Store (CDS). Available at: <https://cds.climate.copernicus.eu/cdsapp#!/home> [Accessed 5th September 2018].
- Crouvi, O., Schepanski, K., Amit, R., Gillespie, A.R. and Enzel, Y. (2012) Multiple dust sources in the Sahara Desert: the importance of sand dunes. *Geophysical Research Letters*, 39(13), 1–8. <https://doi.org/10.1029/2012GL052145>.
- Dolinar, E.K., Dong, X., Xi, B., Jiang, J.H. and Su, H. (2014) Evaluation of CMIP5 simulated clouds and TOA radiation budgets using NASA satellite observations. *Climate Dynamics*, 44, 2229–2247. <https://doi.org/10.1007/s00382-014-2158-9>.
- Fink, A.H., Paeth, H., Ermert, V., Pohle, S. and Diederich, M. (2010) Meteorological processes influencing the weather and climate of Benin. In: Speth, P., Christoph, M. and Dieckrüger, B. (Eds.) *Impacts of Global Change on the Hydrological Cycle in West and NW Africa*. Berlin, Heidelberg: Springer, pp. 135–149. <https://doi.org/10.1007/978-3-642-12957-5>.
- Forbes, R. (2017) *Clouds and precipitation: from models to forecasting. Use and interpretation of ECMWF products* (p. 38). Available at: <https://confluence.ecmwf.int/display/FUG/Clouds>.
- Gbobaniyi, E., Sarr, A., Sylla, M.B., Diallo, I., Lennard, C., Dosio, A., Dhiédiou, A., Kamga, A., Klutse, N.A.B., Hewitson, B., Nikulin, G. and Lamptey, B. (2014) Climatology, annual cycle and interannual variability of precipitation and temperature in CORDEX simulations over West Africa. *International Journal of Climatology*, 34(7), 2241–2257. <https://doi.org/10.1002/joc.3834>.
- Hill, P.G., Allan, R.P., Chiu, J.C., Bodas-Salcedo, A. and Knippertz, P. (2018) Quantifying the contribution of different cloud types to the radiation budget in southern West Africa. *Journal of Climate*, 31(13), 5273–5291. <https://doi.org/10.1175/JCLI-D-17-0586.1>.
- Hill, P.G., Allan, R.P., Chiu, J.C. and Stein, T.H.M. (2016) A multisatellite climatology of clouds, radiation, and precipitation in southern West Africa and comparison to climate models. *Journal of Geophysical Research: Atmospheres*, 121(18), 10,857–10,879. <https://doi.org/10.1002/2016JD025246>.
- Jakob, C. and Klein, S.A. (2000) A parametrization of the effects of cloud and precipitation overlap for use in general-circulation models. *Quarterly Journal of the Royal Meteorological Society*, 126, 2525–2544. <https://doi.org/10.1002/qj.49712656809>.
- Karlsson, K.G. and Johansson, E. (2013) On the optimal method for evaluating cloud products from passive satellite imagery using CALIPSO-CALIOP data: example investigating the CM SAF CLARA-A1 dataset. *Atmospheric Measurement Techniques*, 6(5), 1271–1286. <https://doi.org/10.5194/amt-6-1271-2013>.

- Kasten, F. and Czeplak, G. (1980) Solar and terrestrial radiation dependent on the amount and type of cloud. *Solar Energy*, 24, 177–189.
- Klein, C., Heinzeller, D., Bliefernicht, J. and Kunstmann, H. (2015) Variability of West African monsoon patterns generated by a WRF multi-physics ensemble. *Climate Dynamics*, 45(9–10), 2733–2755. <https://doi.org/10.1007/s00382-015-2505-5>.
- Knippertz, P., Coe, H., Chiu, J.C., Evans, M.J., Fink, A.H., Kalthoff, N., Lioussé, C., Mari, C., Allan, R.P., Brooks, B., Danour, S., Flamant, C., Jegede, O.O., Lohou, F. and Marsham, J.H. (2015) The DAC-CIWA project: dynamics–aerosol–chemistry–cloud interactions in West Africa. *Bulletin of the American Meteorological Society*, 96(9), 1451–1460. <https://doi.org/10.1175/BAMS-D-14-00108.1>.
- Knippertz, P., Fink, A.H., Schuster, R., Trentmann, J., Schrage, J.M. and Yorke, C. (2011) Ultra-low clouds over the southern West African monsoon region. *Geophysical Research Letters*, 38(21), 1–7. <https://doi.org/10.1029/2011GL049278>.
- Knippertz, P. and Todd, M. C. (2012) Mineral dust aerosols over the Sahara: meteorological controls on emission and transport and implications for modeling. *Reviews of Geophysics*, 50(1), 1–28. <https://doi.org/10.1029/2011RG000362>.
- Koren, I., Washington, R., Kaufman, Y.J., Martins, J.V., Todd, M.C., Rudich, Y. and Rosenfeld, D. (2006) The Bodélé depression: a single spot in the Sahara that provides most of the mineral dust to the Amazon forest. *Environmental Research Letters*, 1(1), 014005. <https://doi.org/10.1088/1748-9326/1/1/014005>.
- Lavaysse, C., Flamant, C. and Janicot, S. (2010) Regional-scale convection patterns during strong and weak phases of the Saharan heat low. *Atmospheric Science Letters*, 11, 255–264. <https://doi.org/10.1002/asl.284>.
- Lee, J., Yang, P., Dessler, A.E., Gao, B.-C. and Platnick, S. (2009) Distribution and radiative forcing of tropical thin cirrus clouds. *Journal of the Atmospheric Sciences*, 66(12), 3721–3731. <https://doi.org/10.1175/2009jas3183.1>.
- Liou, K.N. (2002) *An Introduction to Atmospheric Radiation. International Geophysics Series*, 84, 2nd edition. San Diego, CA: Elsevier Science. Retrieved from <https://books.google.fr/books?id=mQ1DiDpX34UC>.
- van der Linden, R., Fink, A.H. and Redl, R. (2015) Satellite-based climatology of low-level continental clouds in southern West Africa during the summer monsoon season. *Journal of Geophysical Research*, 120, 1186–1201. <https://doi.org/10.1002/2014JD022614>.
- Loeb, N.G., Doelling, D.R., Wang, H.L., Su, W.Y., Nguyen, C., Corbett, J.G., et al. (2018) Clouds and the Earth's radiant energy system (CERES) energy balanced and filled (EBAF) top-of-atmosphere (TOA) edition-4.0 data product. *Journal of Climate*, 31(2), 895–918. <https://doi.org/10.1175/JCLI-D-17-0208.1>.
- Lott, N., Baldwin, R. and Jones, P. (2001) *The FCC integrated surface hourly database, a new resource of global climate data*. NCDC Technical Report 2001-01. Available at: <https://doi.org/http://www1.ncdc.noaa.gov/pub/data/techrpts/tr2000101/tr2001-01.pdf>.
- Mace, G.G., Deng, M., Soden, B. and Zipser, E. (2005) Association of tropical cirrus in the 10–15-km layer with deep convective sources: an observational study combining millimeter radar data and satellite-derived trajectories. *Journal of the Atmospheric Sciences*, 63, 480–503. <https://doi.org/10.1175/JAS3627.1>.
- Middleton, N.J. and Goudie, A.S. (2001) Saharan dust: sources and trajectories. *Transactions of the Institute of British Geographers*, 26(2), 165–181. <https://doi.org/10.1111/1475-5661.00013>.
- Miller, M.A. and Slingo, A. (2007) The ARM mobile facility and its first international deployment: measuring radiative flux divergence in West Africa. *Bulletin of the American Meteorological Society*, 88(8), 1229–1244. <https://doi.org/10.1175/BAMS-88-8-1229>.
- Minnis, P., Hong, G., Sun-mack, S., Smith, W.L., Chen, Y. and Miller, S.D. (2016) Estimating nocturnal opaque ice cloud optical depth from MODIS multispectral infrared radiances using a neural network method. *Journal of Geophysical Research: Atmospheres*, 121(9), 4907–4932. <https://doi.org/10.1002/2015JD024456>.
- Minnis, P., Sun-Mack, S., Young, D.F., Heck, P.W., Garber, D.P., Chen, Y., Spangenberg, D.A., Arduini, R.F., Trepte, Q.Z., Smith, W.L., Ayers, J.K., Gibson, S.C., Miller, W.F., Hong, G., Chakrapani, V., Takano, Y., Liou, K.N., Xie, Y. and Yang, P. (2011) CERES edition-2 cloud property retrievals using TRMM VIRS and Terra and Aqua MODIS data. Part I: Algorithms. *IEEE Transactions on Geoscience and Remote Sensing*, 49(11), 4374–4400. <https://doi.org/10.1109/TGRS.2011.2144601>.
- Parker, D.J. and Diop-Kane, M. (2017) *Meteorology of Tropical West Africa: The Forecasters' Handbook*, 1st edition. Chichester: John Wiley & Sons Ltd. <https://doi.org/10.1002/9781118391297>.
- Pyrina, M., Hatzianastassiou, N., Matsoukas, C., Fotiadis, A., Papadimas, C.D., Pavlakis, K.G. and Vardavas, I. (2013) Cloud effects on the solar and thermal radiation budgets of the Mediterranean basin. *Atmospheric Research*, 152, 14–28. <https://doi.org/10.1016/j.atmosres.2013.11.009>.
- Redelsperger, J.-L., Thorncroft, C.D., Diedhiou, A., Lebel, T., Parker, D.J. and Polcher, J. (2006) African monsoon multidisciplinary analysis: an international research project and field campaign. *Bulletin of the American Meteorological Society*, 87(12), 1739–1746. <https://doi.org/10.1175/BAMS-87-12-1739>.
- Sassen, K., Wang, Z. and Liu, D. (2009) Cirrus clouds and deep convection in the Tropics: insights from CALIPSO and CloudSat. *Journal of Geophysical Research*, 114, 1–11. <https://doi.org/10.1029/2009JD011916>.
- Schumacher, C. and Houze Jr, R.A. (2006) Stratiform precipitation production over sub-Saharan Africa and the tropical East Atlantic as observed by TRMM. *Quarterly Journal of the Royal Meteorological Society*, 132(620), 2235–2255. <https://doi.org/10.1256/qj.05.121>.
- Soden, B.J. and Held, I.M. (2005) An assessment of climate feedbacks in coupled ocean–atmosphere models. *Journal of Climate*, 19, 3354–3360. <https://doi.org/10.1175/JCLI3799.1>.
- Söhne, N., Chaboureaud, J.-P. and Guichard, F. (2008) Verification of cloud cover forecast with satellite observation over West Africa. *Monthly Weather Review*, 136(11), 4421–4434. <https://doi.org/10.1175/2008MWR2432.1>.
- Stein, T.H.M., Parker, D.J., Delanoë, J., Dixon, N.S., Hogan, R.J., Knippertz, P., Maidment, R.I. and Marsham, J.H. (2011) The vertical cloud structure of the West African monsoon: a 4 year climatology using CloudSat and CALIPSO. *Journal of Geophysical Research*, 116(22), 1–13. <https://doi.org/10.1029/2011JD016029>.
- Stephens, G., Winker, D., Pelon, J., Trepte, C., Vane, D., Yuhas, C., L'Ecuey, T. and Lebsock, M. (2018) CloudSat and CALIPSO within the A-train: ten years of actively observing the Earth system. *Bulletin of the American Meteorological Society*, 99(3), 569–581. <https://doi.org/10.1175/BAMS-D-16-0324.1>.
- Sun, W., Videen, G., Kato, S., Lin, B., Lukashin, C. and Hu, Y. (2011) A study of subvisual clouds and their radiation effect with a synergy of CERES, MODIS, CALIPSO, and AIRS data. *Journal of Geophysical Research*, 116(22), 1–10. <https://doi.org/10.1029/2011JD016422>.

- Supit, I. and van Kappel, R.R. (1998) A simple method to estimate global radiation. *Solar Energy*, 63(3), 147–160. [https://doi.org/10.1016/S0038-092X\(98\)00068-1](https://doi.org/10.1016/S0038-092X(98)00068-1).
- Sylla, M.B., Giorgi, F., Ruti, P.M., Calmanti, S. and Dell'Aquila, A. (2011) The impact of deep convection on the west African summer monsoon climate: a regional climate model sensitivity study. *Quarterly Journal of the Royal Meteorological Society*, 137(659), 1417–1430. <https://doi.org/10.1002/qj.853>.
- Thorncroft, C.D., Nguyen, H., Zhang, C. and Peyrill, P. (2011) Annual cycle of the West African monsoon: regional circulations and associated water vapour transport. *Quarterly Journal of the Royal Meteorological Society*, 137(654), 129–147. <https://doi.org/10.1002/qj.728>.
- Tiedtke, M. (1993) Representation of clouds in large-scale models. *Monthly Weather Review*, 121, 3040–3061. [https://doi.org/10.1175/1520-0493\(1993\)121<3040:ROCILS>2.0.CO;2](https://doi.org/10.1175/1520-0493(1993)121<3040:ROCILS>2.0.CO;2).
- Vizy, E.K. and Cook, K.H. (2018) Understanding the summertime diurnal cycle of precipitation over sub-Saharan West Africa: regions with daytime rainfall peaks in the absence of significant topographic features. *Climate Dynamics*, 52(5–6), 2903–2922. <https://doi.org/10.1007/s00382-018-4315-z>.
- Wielicki, B.A., Barkstrom, B.R., Harrison, E.F., Lee, R.B., Smith, L.G. and Cooper, J.E. (1996) Clouds and the Earth's radiant energy system

(CERES): an Earth observing system experiment. *Bulletin of the American Meteorological Society*, 77(5), 853–868. [https://doi.org/10.1175/1520-0477\(1996\)077<0853:catere>2.0.co;2](https://doi.org/10.1175/1520-0477(1996)077<0853:catere>2.0.co;2).

Yang, G.-Y. and Slingo, J. (2001) The diurnal cycle in the Tropics. *Monthly Weather Review*, 129(4), 784–801. [https://doi.org/10.1175/1520-0493\(2001\)129<0784:TDCITT>2.0.CO;2](https://doi.org/10.1175/1520-0493(2001)129<0784:TDCITT>2.0.CO;2).

## SUPPORTING INFORMATION

Additional supporting information may be found online in the Supporting Information section at the end of this article.

**How to cite this article:** Danso DK, Anquetin S, Diedhiou A, Lavaysse C, Koba A, Touré NDE. Spatio-temporal variability of cloud cover types in West Africa with satellite-based and reanalysis data. *Q J R Meteorol Soc.* 2019;145:3715–3731. <https://doi.org/10.1002/qj.3651>